Cell

XLF Interacts with the XRCC4-DNA Ligase IV Complex to Promote DNA Nonhomologous End-Joining

Peter Ahnesorg,[1,2] Philippa Smith,[1,2] and Stephen P. Jackson[1,2,*]
[1] The Gurdon Institute
[2] Department of Zoology
Cambridge University, Tennis Court Road, Cambridge, CB2 1QN, United Kingdom
*Contact: s.jackson@gurdon.cam.ac.uk
DOI 10.1016/j.cell.2005.12.031

SUMMARY

DNA nonhomologous end-joining (NHEJ) is a predominant pathway of DNA double-strand break repair in mammalian cells, and defects in it cause radiosensitivity at the cellular and whole-organism levels. Central to NHEJ is the protein complex containing DNA Ligase IV and XRCC4. By searching for additional XRCC4-interacting factors, we identified a previously uncharacterized 33 kDa protein, XRCC4-like factor (XLF, also named Cernunnos), that has weak sequence homology with XRCC4 and is predicted to display structural similarity to XRCC4. We show that XLF directly interacts with the XRCC4-Ligase IV complex in vitro and in vivo and that siRNA-mediated downregulation of XLF in human cell lines leads to radiosensitivity and impaired NHEJ. Furthermore, we establish that NHEJ-deficient 2BN cells derived from a radiosensitive and immune-deficient patient lack XLF due to an inactivating frameshift mutation in its gene, and that reintroduction of wild-type XLF into such cells corrects their radiosensitivity and NHEJ defects. XLF thus constitutes a novel core component of the mammalian NHEJ apparatus.

INTRODUCTION

The DNA double-strand break (DSB) is probably the most cytotoxic cellular lesion known, with as little as one unrepaired DSB being capable of triggering programmed cell death (Rich et al., 2000). DSBs are the principle cytotoxic lesions generated by ionizing radiation (IR) and radiomimetic chemicals, can be caused by mechanical stress on chromosomes, and also arise when DNA replication forks encounter other lesions such as DNA single-strand breaks (Khanna and Jackson, 2001; Mills et al., 2003). Despite posing threats to genomic integrity, DSBs are nonetheless sometimes generated deliberately for a defined biological purpose. A good example of this is provided by V(D)J recombination, which takes place in developing B and T lymphocytes to provide the basis for the antigen binding diversity of the vertebrate adaptive immune system (reviewed in Gellert [2002]). Notably, inefficient or inaccurate repair of programmed or spontaneously arising DSBs can lead to mutations, dicentric or acentric chromosomal fragments and/or chromosomal translocations; and in some cases these have oncogenic potential (Difilippantonio et al., 2002; Ferguson and Alt, 2001; Khanna and Jackson, 2001; Mills et al., 2003).

There are two principle pathways for DNA DSB repair: homologous recombination (HR) and nonhomologous end-joining (NHEJ). These pathways are largely distinct from one another and function in complementary ways to bring about DSB repair (Haber, 2000). During HR, the damaged chromosome enters into synapsis with an undamaged DNA molecule with which it shares extensive sequence homology: usually its sister chromatid (reviewed in Modesti and Kanaar [2001]; West, 2003). By contrast, NHEJ does not require a homologous undamaged partner DNA molecule and moreover does not need extensive sequence homologies between the recombining DNA ends (for reviews see Lieber et al. [2003] and Weterings and Van Gent [2004]). However, while its ability to ligate essentially any two DNA ends makes NHEJ a very effective pathway of DSB repair, some end-processing is normally required before ligation, making NHEJ an intrinsically mutagenic repair mechanism. Reflecting the key importance of the NHEJ apparatus, mammalian cells bearing defects in core NHEJ components exhibit pronounced hypersensitivity toward IR and other agents that cause DSBs but not toward agents that yield other types of DNA lesions (reviewed in Lieber et al. [2004]). When such NHEJ defects are manifested at the whole-animal level, they are also usually associated with defective V(D)J recombination and/or immunoglobulin class-switch recombination, causing

severe combined immune-deficiency or related immunodeficiencies (Ferguson and Alt, 2001; Lieber et al., 2004).

At the heart of the NHEJ apparatus in all eukaryotes studied is the enzyme DNA Ligase IV, which directly mediates DNA-strand joining by this pathway (Robins and Lindahl, 1996). In addition to possessing a canonical DNA ligase catalytic domain, Ligase IV is distinct from other eukaryotic DNA ligases in that it possesses two tandem C-terminal BRCT domains. A key development in our understanding of Ligase IV was the discovery that it exists in a tight complex with the ~38 kDa ''adaptor'' protein XRCC4 (Critchlow et al., 1997; Grawunder et al., 1997; Herrmann et al., 1998), deficiency in which also causes marked NHEJ defects (Li et al., 1995). Structural studies have revealed that XRCC4 contains a globular N-terminal ''head'' domain—which might interact with other proteins and/or DNA—and a protruding helical coiled-coil region that contains a motif that interacts directly with the linker region between the two BRCT domains of Ligase IV (Grawunder et al., 1998b; Junop et al., 2000; Sibanda et al., 2001). XRCC4 is tightly associated with Ligase IV in vivo and is required for its stability (Bryans et al., 1999). Furthermore, it has been shown that XRCC4 stimulates Ligase IV adenylation and overall activity in vitro and in vivo (Grawunder et al., 1997; Grawunder et al., 1998a; Modesti et al., 1999). Subsequently, it was shown that targeted inactivation of the genes for Ligase IV or XRCC4 in mouse cells leads to radiosensitivity and NHEJ defects (Barnes et al., 1998; Frank et al., 1998) and that human patients with inherited hypomorphic mutations in Ligase IV are radiosensitive and also display varying degrees of immune deficiency (O'Driscoll et al., 2001; Riballo et al., 1999).

A striking feature of the Ligase IV-XRCC4 complex is that it functions in NHEJ but not in other DNA repair pathways. This specificity reflects the fact that, despite having an intrinsic capability to bind DNA, the XRCC4-Ligase IV complex is ineffective at recognizing DSBs alone and needs to be physically recruited to these sites by other NHEJ components (McElhinny et al., 2000; Teo and Jackson, 2000). Two such proteins are the heterodimeric DNA-end binding protein Ku and the DNA-dependent protein kinase catalytic subunit (DNA-PKcs), with which Ku associates (Smith and Jackson, 1999). The Ku heterodimer forms a ring-like structure, which binds to DNA ends and has been proposed to initiate the NHEJ process. Upon DNA-PKcs recruitment, Ku translocates inward and potentially allows DNA-PKcs to bridge the broken DNA ends and promote ligation by Ligase IV-XRCC4 (reviewed in Hefferin and Tomkinson [2005]). Indeed, the XRCC4-Ligase IV complex can interact with Ku and DNA-PKcs in vitro (Chen et al., 2000; Hsu et al., 2002; Kysela et al., 2003), and XRCC4 is phosphorylated by DNA-PKcs, although any functional relevance for this phosphorylation event remains elusive (Critchlow et al., 1997; Leber et al., 1998). Other proteins implicated in mammalian NHEJ are as follows: Artemis, whose nuclease function is thought to aid the processing of V(D)J recombination intermediates and certain radiation-induced lesions before they are ligated (Moshous et al., 2001); DNA polymerases of the Pol X family that are thought to mediate strand-filling steps in the pathway (for example, Ma et al. [2004]); and polynucleotide kinase that modifies certain DNA terminal structures to permit their subsequent ligation (Chappell et al., 2002; Koch et al., 2004).

Although the above factors seem in principle capable of carrying out all the known steps of NHEJ and promote ligation in vitro, it has recently become apparent that at least one additional core NHEJ component in vivo remains to be identified. Thus, work on 2BN cells—derived from a radiosensitive and immune-deficient patient—has revealed them to display a marked NHEJ deficiency that cannot be ascribed to defects in any of the known NHEJ components (Dai et al., 2003). With this in mind, we carried out searches for factors that bind to established NHEJ components. Herein, we describe the identification of one such human protein, XLF, and demonstrate that it not only corresponds to a new core NHEJ component but is, in fact, the factor mutated in 2BN cells. Based on our biochemical observation that XLF interacts with the Ligase IV-XRCC4 complex and our findings that XLF is required for efficient repair of DNA DSBs in vivo, we discuss the likely mechanisms by which XLF promotes effective DSB repair in mammalian cells.

RESULTS

Yeast Two-Hybrid Screening for XRCC4 Interactors

Due to the pivotal role of XRCC4 in NHEJ, we searched for further XRCC4-interacting proteins. Thus, we conducted a LexA-based yeast two-hybrid screen with full-length XRCC4 as bait (see Experimental Procedures for details). The screen yielded 78 positive clones, out of which we have currently examined 25. Two of these positive and bait-dependent cDNA clones encoded Aprataxin, which has recently been reported to interact with XRCC4 (Clements et al., 2004). Two further cDNA clones corresponded to N-terminal portions of an as-yet-uncharacterized human open reading frame (*FLJ12610*) that encodes a predicted full-length protein of ~33 kDa (Figure 1A). As shown in Figure 1B, the 299 residue FLJ12610 protein is well conserved throughout vertebrate species, with stretches of particularly high sequence conservation in its N-terminal region (residues 34–79) and its middle portion (residues 120–205). The encoded protein also contains a putative nuclear localization sequence at its very C terminus (KRKK).

XLF (FLJ12610) Is Predicted to Display Structural Similarity to XRCC4

Standard sequence homology and motif searches failed to identify any FLJ12610-related proteins other than the family of its vertebrate orthologs. Strikingly, however, sequence structure comparisons with either the Fugue algorithm (http://www-cryst.bioc.cam.ac.uk/~fugue/; Shi et al., 2001) or the 3D-PSSM algorithm (Fold recognition server, http://www.sbg.bio.ic.ac.uk/~3dpssm/; Kelley et al., 2000) indicated that the FLJ12610 protein very likely displays a similar structural organization to XRCC4 (Figure 1C; see Table S1 and Figure S1 in the Supplemental Data available with this article online). Indeed, when FLJ12610 and its vertebrate

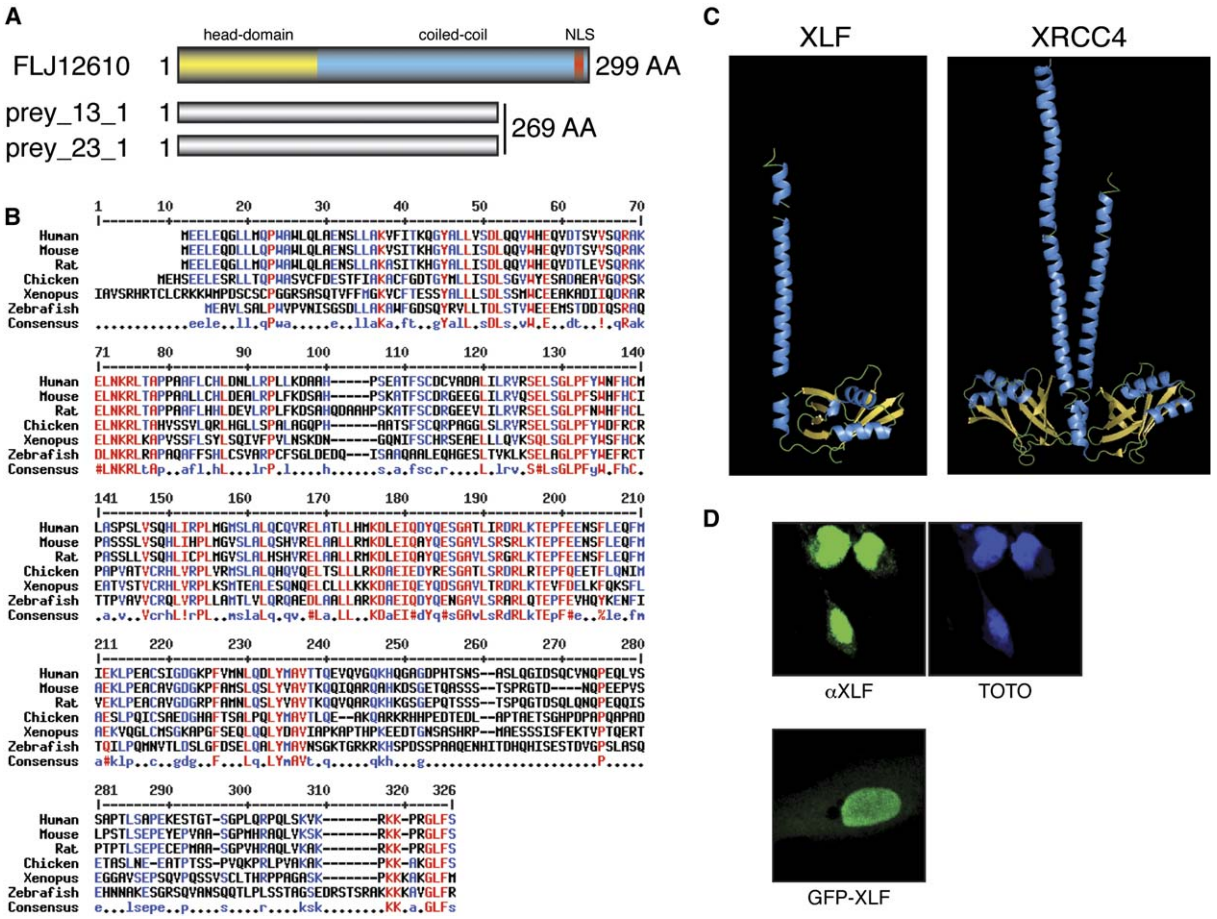

Figure 1. XLF, a Conserved 33 kDa Protein, Interacts with XRCC4 in a Yeast Two-Hybrid Screen and Is Predicted to Show Structural Similarity to XRCC4

(A) Schematic representation of full-length XLF and two cDNA clones identified from a yeast-two hybrid screen with full-length XRCC4 as bait. Out of 75 interacting clones, two (gray) were identified as encoding the N-terminal region of FLJ12610 (XLF). Above is a representation of full-length XLF, with predicted head, coiled-coil, and nuclear localization sequence (NLS) indicated.

(B) XLF is conserved throughout vertebrates. Alignment (Multalin, http://prodes.toulouse.inra.fr/mutalin/mutalin.html) of human XLF (FLJ12610) and homologs in other representative eukaryotes.

(C) XLF is predicted to display structural homology to XRCC4. Left: comparative structural modeling of the XLF secondary structure based on the structure of XRCC4 (PDB: 1fu1 and 1ik9, http://swissmodel.expasy.org/). Right: XRCC4 dimer structural coordinates (PDB: 1fu1) visualized using MacPyMOL.

(D) XLF localizes to the nucleus. Confocal images: top, U2OS cells were fixed and stained with rabbit anti-XLF polyclonal antibody, together with TOTO3 dye to visualize DNA. Bottom, U2OS cells were transfected with GFP-XLF and fixed 24 hr afterwards.

family members were compared to the secondary structure and fold databases of these algorithms, FLJ12610 homologs were predicted with high confidence to adopt a fold similar to the structure solved for XRCC4 (Fugue, Z score 4.75 and 4.0, 95% confidence; 3D-PSSM, E value 0.027, 95% confidence). Specifically, this analysis suggested that, like the similarly-sized XRCC4 protein, FLJ12610 encodes a protein containing an N-terminal "head" domain, with the remainder of the protein adopting a coiled-coil structure (Figure 1C). In line with these predictions, sequence comparisons revealed a low level of sequence similarity between FLJ12610 and XRCC4, particularly in the region of XRCC4 that is believed to interact with Ligase IV. In light of these findings and our other data linking FLJ12610 to XRCC4 (see below), we have given it the name "XRCC4-like factor" (XLF).

XLF Is a Nuclear Protein Expressed in Human Cell Lines

To further study XLF, we raised a rabbit polyclonal antibody against the full-length recombinant protein and used this to examine XLF expression. Thus, we established that XLF is present in a wide range of human cell lines (Figure 4B and data not shown). Furthermore, indirect immunofluorescence staining revealed that XLF, like XRCC4, localizes primarily to the nucleus of human cells (Figure 1D, top). Consistent

with these findings, we found that a green fluorescent protein (GFP)-XLF fusion was primarily nuclear (Figure 1D, bottom).

XLF Interacts with XRCC4 and DNA Ligase IV In Vitro and In Vivo

The identification of XLF by a yeast two-hybrid screen for XRCC4 interactors suggested that XLF might functionally cooperate with the XRCC4-DNA Ligase IV complex. To begin to explore this possibility, we generated a glutathione S-transferase (GST)-XLF fusion protein in bacteria, purified this, and then used it in protein interaction studies. Thus, we found that GST-XLF efficiently retrieved both XRCC4 and Ligase IV from HeLa nuclear extract (HNE), whereas it did not bind the DNA repair and checkpoint factor Mre11 (Figure 2A) nor various other proteins analyzed (Rad50, DNA-PKcs, and SMC1; data not shown). These interactions between XLF and the XRCC4-Ligase IV were unlikely to be mediated by small amounts of DNA in the extract, as the experiments were carried out in the presence of 50 μg/ml ethidium bromide, which disrupts the majority of protein-DNA interactions. Furthermore, we found that GST-XLF pull-downs can quantitatively deplete extracts of virtually all XRCC4 and Ligase IV (data not shown).

To test whether XLF can interact with the XRCC4-Ligase IV complex in vivo, we transfected 293T cells with a vector directing the expression of HA epitope-tagged XLF, made extracts from these, and tested for the presence of HA-XLF, XRCC4, and Ligase IV in anti-HA immunoprecipitates. As shown in Figure 2B, XRCC4 and Ligase IV indeed coimmunoprecipitated with HA-XLF but were not present in control immunoprecipitates with anti-GFP antibodies, nor were they found in HA-immunoprecipitates from extracts of cells transfected with the parental vector (pCDNA3.1). Moreover, we established that endogenous XLF in HNE is associated with XRCC4 (Figure 2C) and Ligase IV (Figure 2D), as both these proteins were specifically coimmunoprecipitated with the rabbit anti-XLF antibody. The XRCC4-XLF interaction was also confirmed in reciprocal immunoprecipitations with a mouse anti-XRCC4 antibody (Figure 2E). Interestingly, we found as a result of cotransfection studies that HA-tagged XLF could be immunoprecipitated with an anti-FLAG epitope-tag antibody when it was expressed in cells together with FLAG-tagged XLF (Figure 2F; no HA-XLF was precipitated by anti-FLAG antibody in the absence of FLAG-XLF; data not shown). This suggests that multiple XLF proteins interact with the XRCC4-Ligase IV complex and/or that XLF can exist as multimers, as is the case for XRCC4 itself (Junop et al., 2000; Lee et al., 2000; Modesti et al., 2003). Taken together, the above data reveal that XLF behaves as a bona fide component of the XRCC4-Ligase IV complex.

Downregulation of XLF in Human Cell Lines Causes Marked Radiosensitivity

In light of the above data, we speculated that XLF might be involved in the NHEJ pathway of DSB repair. To test this idea, we developed two independent siRNA double-stranded oligonucleotides that target XLF—XLFsi(1) and XLFsi(2)—and showed that each was capable of efficiently downregulating XLF protein levels in human U2OS cells (Figure 3A, top and bottom panels). As a control for subsequent studies, we used an siRNA oligonucleotide that efficiently downregulated XRCC4 (Figure 3A, top). Downregulation of XRCC4 also led to decreased Ligase IV levels, which confirms previous reports indicating that XRCC4 is required for normal Ligase IV protein stability (Bryans et al., 1999; Teo and Jackson, 2000). Strikingly, we found that cells downregulated for XLF were markedly more radiosensitive than cells downregulated with control siRNA oligonucleotides (Figure 3B). Moreover, the radiosensitivity of XLF-depleted cells was equivalent to that of cells downregulated for XRCC4 (Figure 3B). In line with the above findings, we found that downregulation of XLF also sensitized cells to Bleocin, a drug that generates a high yield of DNA DSBs; and again, the degree of sensitization caused by XLF depletion was similar to that achieved by XRCC4 downregulation (Figure 3C). Taken together, these results indicate that XLF is required for cellular survival in response to DSB-generating agents and furthermore support the contention that XLF and XRCC4 function in the same pathway.

Downregulation of XLF in Human Cell Lines Causes a Defect in DNA DSB Repair

NHEJ is a predominant DSB pathway in mammalian cells and is crucial for the efficient random integration of plasmid DNA into the genome of human tissue culture cells (Lou et al., 2004). Consistent with this, we found that random plasmid integration was markedly impaired in cells downregulated for XRCC4 (Figure 3D). Moreover, downregulation of XLF reduced integration efficiencies to levels comparable to those caused by XRCC4 depletion (Figure 3D). These findings strongly suggested that XLF, like XRCC4, is crucial for DNA DSB repair by NHEJ. To verify this, we used pulsed-field gel electrophoresis (PFGE) to monitor the repair of IR-induced DSBs in vivo. Thus, we transfected U2OS cells with siRNAs targeting XLF, XRCC4, or GFP, and after allowing time for protein downregulation, we treated the cells with 80 Gy of IR. While cells transfected with the control siRNA were able to repair most DSBs quickly after irradiation (loss of the faster-migrating DNA signal), cells downregulated for XLF or XRCC4 displayed much higher levels of broken DNA molecules migrating into the gel, and this was the case both at early and later time points (Figure 3E). These data therefore indicate that both XLF and XRCC4 are required for normal DNA NHEJ as measured by this assay.

To further study the requirement of XLF for DSB repair, we analyzed the phosphorylation of histone H2AX on Ser 139 (γH2AX) in response to IR. It has previously been established that phosphorylation of H2AX correlates with DSB formation (Rogakou et al., 1998) and that by measuring the extent of phosphorylation or nuclear foci formation of γH2AX after radiation, one can obtain a fairly accurate assessment of the extent of DSB repair (for example, Kuhne et al. [2004], Mirzoeva and Petrini [2001], Rothkamm and Lobrich [2003]). While phosphorylated H2AX was readily detectable 2 hr after

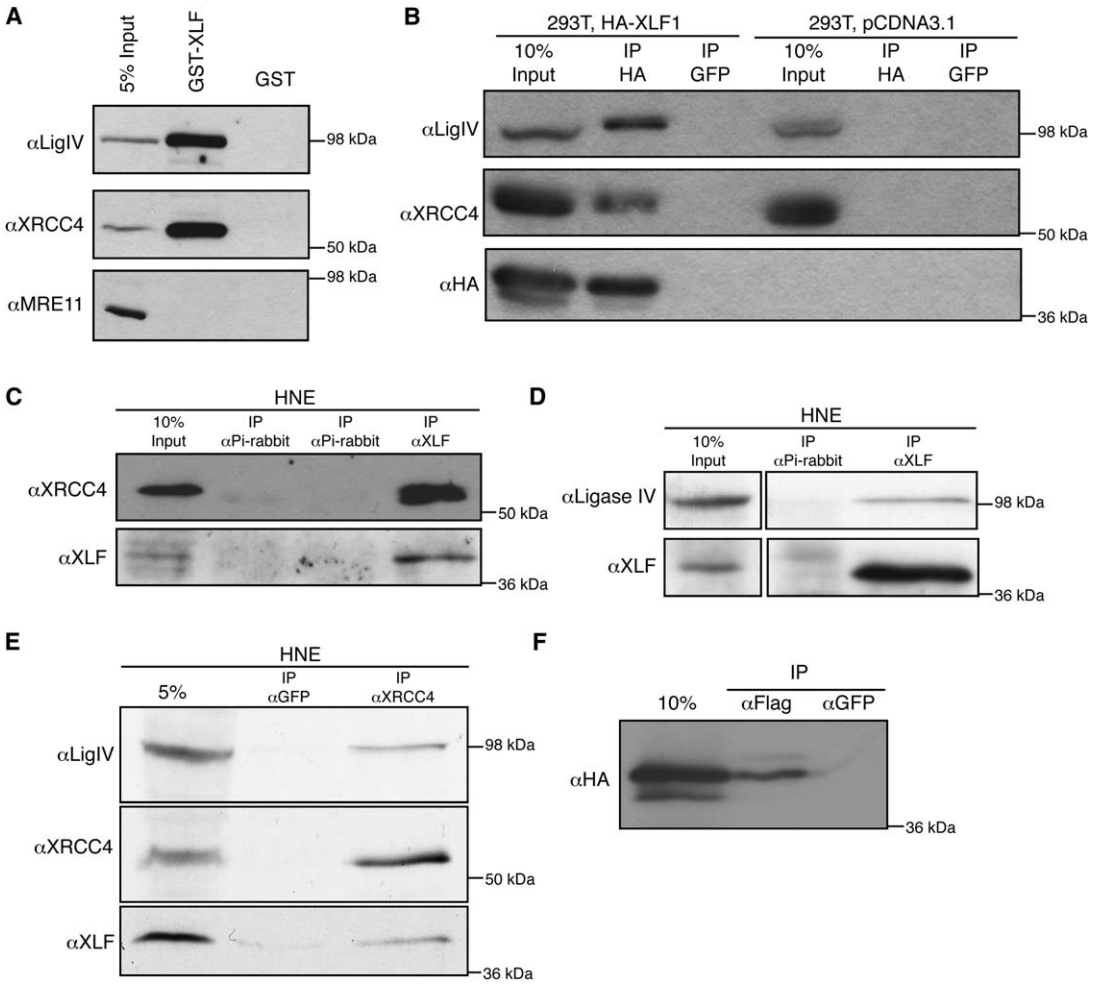

Figure 2. XLF Interacts with the XRCC4-Ligase IV Complex In Vitro and In Vivo

(A) GST-XLF interacts with XRCC4 and Ligase IV in pull-down experiments. GST pull-downs from 800 μg of HeLa cell nuclear extract (HNE). Purified GST-XLF or GST alone was bound to glutathione-Sepharose and incubated with HNE in the presence of 50 μg/ml ethidium bromide. Washed beads were analyzed by immunoblotting with rabbit anti-Ligase IV, rabbit anti-XRCC4, and rabbit anti-MRE11 antibodies, as indicated. Five percent of input material was analyzed as a control.

(B) HA-XLF interacts with XRCC4 and Ligase IV in 293T cells. Coimmunoprecipitation of XRCC4 and Ligase IV with HA-XLF from 1 mg of 293T whole-cell extract (WCE). 293T cells were transfected with HA-XLF or empty vector control (pCDNA3.1). Extracts were prepared 20 hr after transfection and precipitated with monoclonal mouse anti-HA or mouse anti-GFP antibody. Samples were analyzed by immunoblotting with rabbit anti-Ligase IV, rabbit anti-XRCC4, and rabbit anti-HA antibodies, as indicated. Ten percent of input material was analyzed as a control.

(C) Endogenous XLF interacts with XRCC4 in HNE. Coimmunoprecipitation of XRCC4 with XLF from 1 mg of HNE. For immunoprecipitation, rabbit preimmune (Pi) serum or rabbit anti-XLF (α-XLF) antibody was used. Samples were analyzed by immunoblotting with mouse anti-XRCC4 and affinity purified rabbit anti-XLF antibody, as indicated. Ten percent of input material was analyzed as a control.

(D) Endogenous XLF interacts with Ligase IV in HNE. Coimmunoprecipitation of Ligase IV with XLF from 1 mg of HNE. For immunoprecipitations, rabbit preimmune serum or rabbit anti-XLF antibody was used. Samples were analyzed by immunoblotting with rabbit anti-Ligase IV and affinity purified rabbit anti-XLF antibodies, as indicated. To prevent unspecific crossreactions between the rabbit antibodies, HRP-conjugated protein A was used as secondary reagent. Ten percent of input material was analyzed as a control.

(E) XRCC4 interacts with endogenous XLF in HNE. Coimmunoprecipitation of XLF with XRCC4 from 5 mg of HNE. For precipitations, mouse anti-XRCC4 antibody or mouse anti-GFP antibody were used. Samples were analyzed by immunoblotting using rabbit anti-Ligase IV, rabbit anti-XRCC4, and affinity-purified rabbit anti-XLF antibody.

(F) XLF can form multimeric complexes. Coimmunoprecipitation of HA-XLF with FLAG-XLF. 293T cells were cotransfected with HA-XLF and FLAG-XLF, and extracts were prepared 20 hr after transfection. For precipitations from 1 μg of WCE, mouse anti-FLAG antibody or mouse anti-GFP antibody was used. Samples were analyzed by immunoblotting using affinity-purified HA-HRP conjugated antibody.

irradiation in cells transfected with control GFP siRNA oligonucleotides, it disappeared quickly thereafter, and virtually no phosphorylated H2AX was detected at later time points (Figure 3F). In contrast, cells downregulated for XLF showed increased levels of H2AX phosphorylation at later time points, indicating that DSBs are less efficiently repaired in

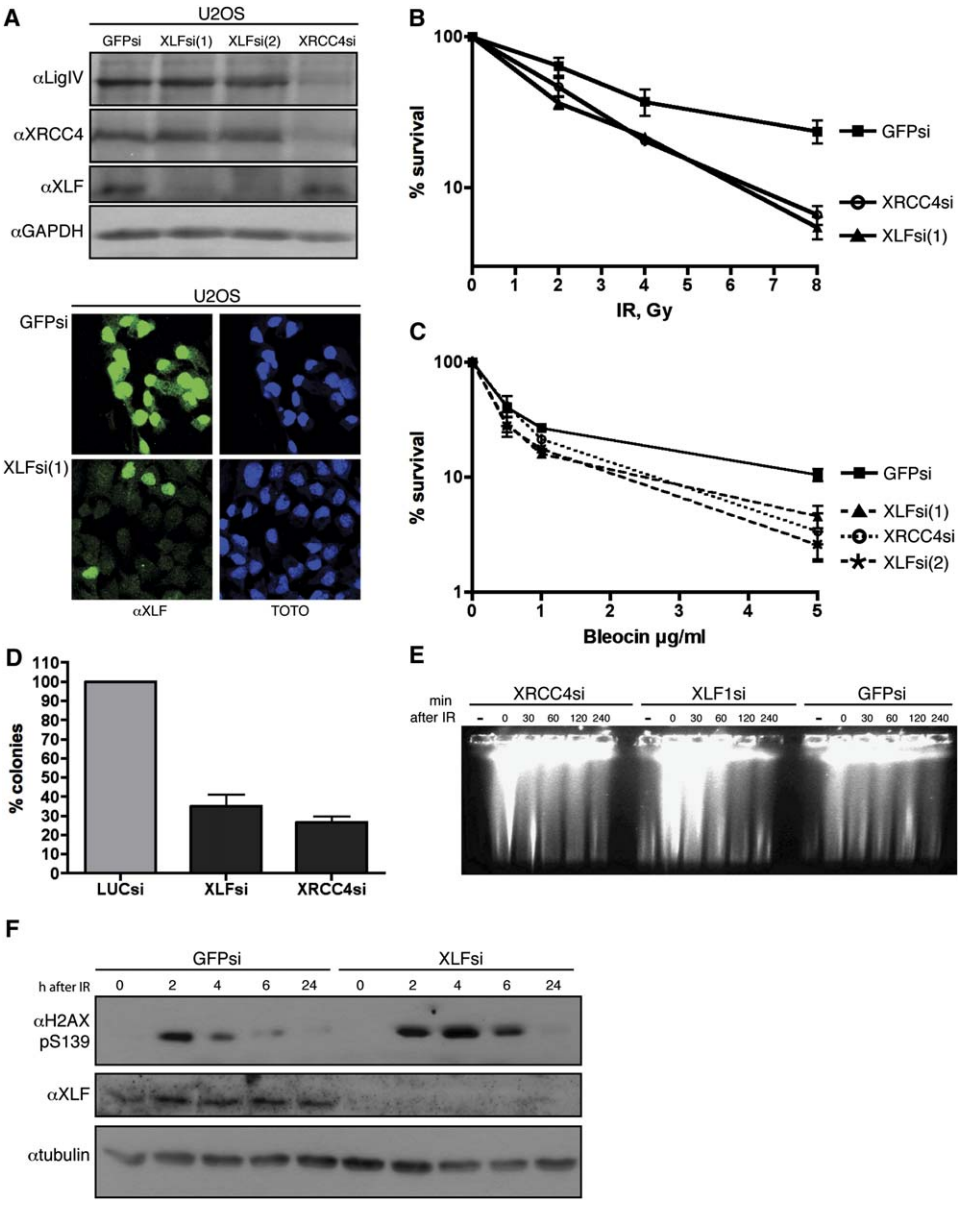

Figure 3. Downregulation of XLF in U2OS Cells Leads to Increased Radiosensitivity, DSB Repair Defects, and Prolonged Phosphorylation of Histone H2AX

(A) siRNA-mediated downregulation of XLF and XRCC4 in U2OS cells. Top: cells were transfected with siRNA oligonucleotides and extracts were prepared 72 hr afterwards. Samples were analyzed by immunoblotting with the indicated antibodies. XLFsi(1) and XLFsi(2) are two independent siRNA oligonucleotides targeting different regions in the XLF1 open reading frame. GFPsi is a control oligonucleotide targeting GFP. Bottom: U2OS cells were treated with XLF siRNA or control (GFPsi) siRNA; 72 hr later, cells were fixed and stained with rabbit anti-XLF rabbit polyclonal antibody, together with TOTO3 dye to visualize DNA. Cells retaining XLF nuclear staining in the bottom left panel presumably escaped XLF downregulation.

(B) XLF downregulation causes radiosensitivity. Clonogenic survival of U2OS cells transfected with GFPsi (■), XLFsi(1) (▲), or XRCC4si (○). Cells were treated with the indicated doses of IR. Data points represent the mean and standard deviation of three independent experiments.

(C) Downregulation of XLF causes hypersensitivity toward the DSB-generating agent, Bleocin. Clonogenic survival of U2OS cells transfected with GFPsi (■), XLFsi(1) (▲), or XLFsi(2) (asterisk) or XRCC4si (○). Cells were treated with the indicated doses of Bleocin for 24 hr. Data represent the mean and standard deviation of three independent experiments.

(D) Downregulation of XLF or XRCC4 causes a marked defect in random plasmid integration. U2OS cells were transfected with indicated siRNA oligonucleotides 24 hr before transfection with pEYFP-Nuc(Kan^r/Neo^r); 24 hr later, the cells were replated at low density in selective medium, and colonies were counted 10 days later. Data represent mean and standard deviation of three independent experiments. Values are given as percentages of the integration efficiency of cells treated with the control Luc siRNA.

the absence of XLF (Figure 3F). Together, these results show that XLF, like XRCC4, is required for the efficient repair of DSBs in human cells.

2BN Cells Derived from a Radiosensitive Patient Lack Detectable XLF Protein

Until a pivotal report by Jeggo and colleagues in 2003 (Dai et al., 2003), it was widely believed that all factors involved in the core process of NHEJ had already been identified. Surprisingly, this report showed that the 2BN cell line derived from a radiosensitive and immune-deficient patient exhibited all the hallmarks of NHEJ deficiency yet did not appear to have a defect in any of the established NHEJ components. This led to the conclusion that 2BN cells are defective in an additional, as-yet-uncharacterized NHEJ protein. To see whether XLF might correspond to this factor, we first carried out indirect immunofluorescence staining of 2BN and control MRC5 or BJ fibroblasts with the anti-XLF antibody. Notably, while nuclear XLF immunostaining was observed in MRC5 and BJ cells, this was not the case for 2BN cells (Figure 4A). Consistent with these findings, immunoblotting studies detected XLF protein in extracts of various human cell lines but not in extracts of 2BN cells (Figure 4B). We did, however, find less XLF in fibroblasts (MRC5 and BJ) than in other standard cell lines (293T and U2OS). In addition, we were unable to detect any XLF in IP-Western studies with the rabbit anti-XLF antibody and extracts prepared from 2BN cells (data not shown). Thus, we conclude that 2BN cells contain no XLF, or only very low levels of the protein.

2BN Cells Bear an Inactivating Mutation in the *XLF* Gene

The above findings raised the possibility that 2BN cells contain a mutation in the *XLF* gene. To see whether this was indeed the case, we prepared mRNA from telomerized 2BN cells (2BN-hTERT cells) and amplified the *XLF* mRNA by RT-PCR. As shown in Figure 4C, although an ~900 bp PCR product was generated from all cell lines tested, we consistently obtained less product from 2BN cells than from the other cell lines, possibly indicating a defect in *XLF* expression or mRNA stability (such as resulting from nonsense-mediated mRNA decay). To explore this further, we cloned *XLF* cDNAs derived from two independent 2BN mRNA preparations and sequenced five clones per preparation. Strikingly, in every one of these sequencing reactions, there was a thymine insertion in the fourth codon of the *XLF* open reading frame (Figure 4C). By contrast, no mutations were ever observed in the *XLF* open reading frame when we analyzed PCR products generated from other cell lines (MRC5, 180BR, MO59J, 1BR, and U2OS; data not shown). To verify these results, we subsequently amplified the first coding exon of the *XLF* gene (exon 11, Figure 4D) from total genomic DNA of 2BN and MRC5 cells. Amplified DNA was cloned and subjected to sequence analysis. Again, while all clones derived from MRC5 cells corresponded to the published *XLF* (*FLJ12610*) genomic sequence, every one of the clones derived from 2BN cells contained the T insertion (Figure 4D, chromatograms). We therefore conclude that 2BN cells either bear this mutation in a homozygous state or carry this mutation on one *XLF* allele, with the other *XLF* allele being deleted. Crucially, the single base-pair insertion mutation in 2BN cells results in a translational frameshift in the *XLF* coding sequence (Figure 4C), leading to an early STOP at the 139th base by shifting the codon from GAA (Glu) to TGA (STOP). As a consequence, the mutated gene is predicted to encode a protein of just 46 amino acid residues, with only the first four of these matching those of the wild-type 299 residue XLF protein (Figures 4C and 4D). This is therefore in line with our inability to detect XLF protein in 2BN extracts and suggests strongly that 2BN cells are functionally null for XLF. Nevertheless, we note that there are alternative START codons downstream of the frameshift mutation, which in theory could lead to the production of proteins corresponding to N-terminally deleted forms of XLF (see Discussion).

Reintroduction of XLF into 2BN Cells Eliminates Their Radiosensitivity

To test whether the severe radiosensitivity of 2BN cells was indeed due to the *XLF* mutation, we established cell lines by introducing the full-length wild-type *XLF* cDNA into 2BN cells by genomic integration. The 2BN-C237 and 2BN-C231 clones thus generated were each derived from a single cell colony and were indistinguishable from 2BN-hTERT cells in morphology, growth rate, and in the levels of expression of various proteins tested (Ligase IV, XRCC4, Tubulin, and GAPDH; data not shown). In contrast to 2BN cells, however, nuclear XLF was readily detected in 2BN-C237 and 2BN-C231 cells (Figure 5A and data not shown). The level of XLF protein expression in 2BN-C237 cells was approximately equivalent to that in various nonfibroblast human cell lines studied (U2OS, HeLa, and 293T; data not shown) although it was higher than that of MRC5 or BJ fibroblasts (Figure 5B, top). Furthermore, and consistent with the data from other cell lines, we found that Ligase IV was coimmunoprecipitated with XLF from extracts of 2BN-C237 cells but was not detected in immunoprecipitates from 2BN cells (Figure 5B, bottom). Most importantly, clonogenic survival assays after treating cells with varying doses of IR revealed that 2BN-C237 and 2BN-C231 cells were dramatically less radiosensitive than 2BN cells (Figure 5C and data not shown). Indeed, following exposure to 2 Gy, less than 10%

(E) Downregulation of XLF leads to a defect in chromosomal DSB repair. Ethidium bromide-stained pulsed-field gel electrophoresis of U2OS cells that had been treated with the indicated siRNA oligonucleotides and irradiated 72 hr afterwards. Cells were irradiated for 40 min at 1.8 Gy/min on ice and left for the indicated amount of time to repair at 37ºC. Then ~100,000 cells were loaded per well and the gel was run at 33V, 50–5000 s linear switch time for 66 hr. (F) Downregulation of XLF causes prolongation of histone H2AX phosphorylation after irradiation. Cells were transfected with XLFsi(1) or GFPsi and then irradiated with 5 Gy of IR 72h afterwards. Extracts were prepared at the indicated time points and were analyzed by immunoblotting with mouse anti-phospho-Ser 139 H2AX antibody.

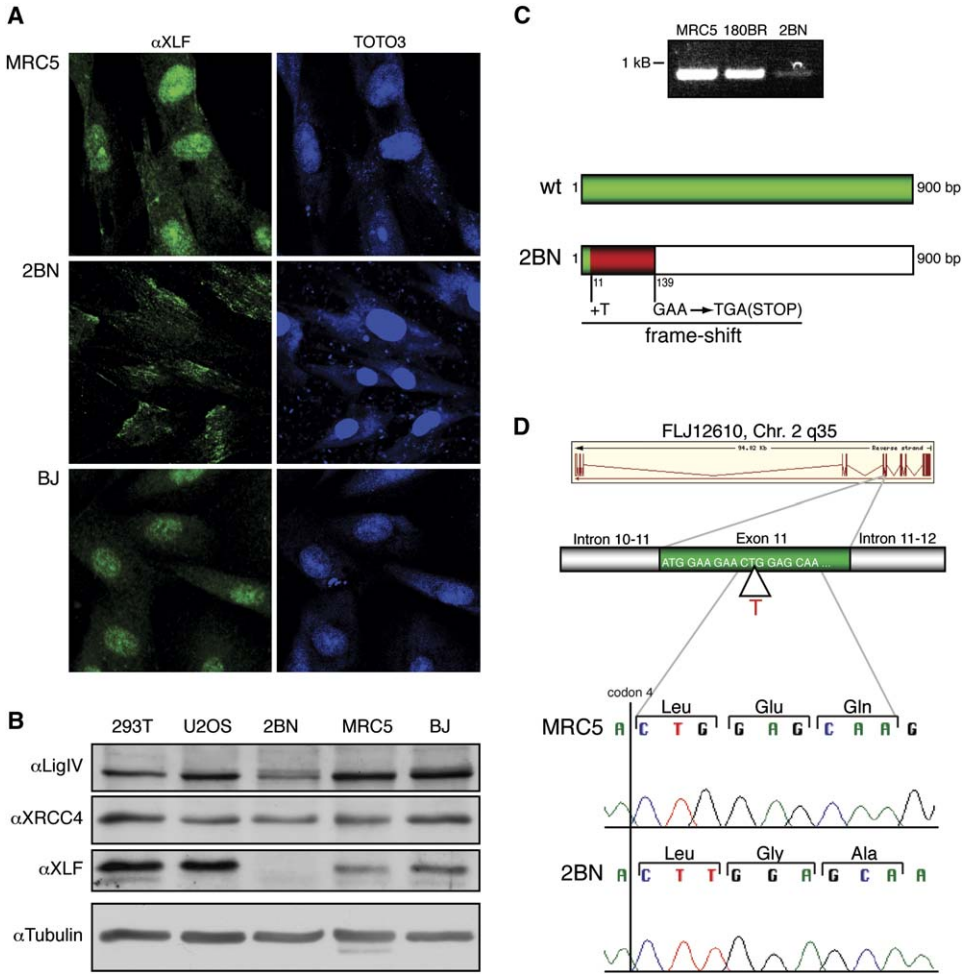

Figure 4. 2BN Cell Line Derived from a Radiosensitive and Immune-Deficient Patient Possesses a Frameshift Mutation in the *XLF* Gene, and XLF Protein Cannot Be Detected in These Cells

(A) Nuclear XLF is not detected by immunofluoresence staining of 2BN cells. Immunofluorescence microscopy of MRC5 (top), 2BN (middle), and BJ (bottom) cells. Cells were stained with rabbit anti-XLF antibody, together with TOTO3 to detect DNA.

(B) No XLF is detectable in 2BN cells by immunoblotting. XLF protein levels in 293T, U2OS, 2BN, MRC5, and BJ cells. Fifty micrograms of RIPA-WCE were analyzed by immunoblotting with rabbit anti-Ligase IV, rabbit anti-XRCC4, rabbit anti-XLF, and rat anti-tubulin antibodies, as indicated.

(C) XLF mRNA from 2BN cells harbors a frameshift mutation. Top: RT-PCR with primers flanking the XLF open reading frame. cDNA was prepared from total mRNA derived from the indicated cell lines and subject to PCR analysis. Bottom: schematic representation of the *XLF* mRNA in wild-type (wt) and 2BN cells.

(D) In 2BN cells, the *XLF* gene is mutated. Top: schematic representation of the *XLF* gene (http://www.ensembl.org) and the first coding exon. Bottom: chromatograms from sequencing reactions of *XLF* exon 11 in samples derived from MRC5 and 2BN cells, as indicated.

of 2BN cells survived while 2BN-C237 and 2BN-231 cells, much like normal fibroblasts (BJ) and U2OS cells, had a survival rate of ~90%. These results therefore confirm that XLF is critical for cellular resistance toward IR and moreover establish that the radiosensitivity of 2BN cells is caused by an XLF defect.

XLF-Complemented 2BN Cells Are Proficient in DNA DSB Repair

To establish whether the introduction of functional XLF into 2BN cells also corrected their DSB repair deficiency, we studied the formation of phosphorylated histone H2AX (γH2AX) in response to IR in 2BN and XLF-complemented 2BN-C237 cells. We observed that noncomplemented 2BN cells had high background levels of γH2AX foci even in the absence of irradiation, suggesting that they are unable to effectively repair spontaneously arising DSBs. By contrast, XLF complemented 2BN-C237 cells exhibited foci levels that were equivalent to those of NHEJ-proficient MRC5 cells (Figures 5D and 5E and data not shown). Moreover, rates of DSB repair as assessed by the disappearance of γH2AX foci took place as effectively in 2BN-C237 cells as in NHEJ-proficient MRC5 cells (Figure 5E). By contrast, 2BN cells displayed high levels of IR-induced γH2AX foci, and no reduction was observed in the first 6 hr of the time course studied after irradiation (Figure 5E). These findings are

consistent with previous work showing that the NHEJ apparatus plays a key role in DSB repair, particularly in the early component of DSB repair events (Iliakis et al., 2004). Furthermore, they reveal that the NHEJ defect of 2BN cells is indeed corrected by XLF expression. Nevertheless, we note that that at longer time points after IR, the extent of γH2AX foci did return to near background levels in all cells tested, suggesting that even in 2BN cells many of the DSBs can eventually be repaired. Presumably this repair is independent of the canonical end-joining process and is mediated by alternative DSB repair pathways irrespective of XRCC4, Ligase IV, or XLF (Wang et al., 2005). Finally, and in accord with the above data, we established by analysis of DSB repair by pulsed-field gel electrophoresis that 2BN cells display a defect in repairing IR-induced DSBs and that this defect is corrected in XLF-complemented 2BN-C237 cells (Figure 5F, gel and graph). We therefore conclude that the DSB repair defect of 2BN cells is a consequence of impaired XLF function.

DISCUSSION

Here, we have described the identification of a previously uncharacterized protein, XLF, as a key component of the mammalian DNA NHEJ apparatus. Thus, we have shown that cells downregulated for XLF display radiosensitivity and defective DNA DSB repair. Furthermore, we have shown that 2BN cells derived from a radiosensitive human patient with immune deficiencies contain a frameshift mutation in the gene for XLF, and that the restoration of wild-type XLF expression to such cells corrects their DSB repair and radiosensitivity phenotypes. As reported elsewhere in this issue of *Cell*, Buck et al. (2006) independently identified the same gene, which they have given the name *Cernunnos*, as being defective in a group of immune-deficient patients with developmental abnormalities. Taken together, these findings demonstrate that XLF/Cernunnos executes a crucial function(s) in DNA NHEJ. In addition, they establish that inherited deficiency in XLF represents a new type of DNA repair syndrome in man.

Although XLF could in principle influence NHEJ indirectly, such as by modulating transcription or other aspects of cell function in ways that facilitate NHEJ, our data strongly argue that the effects of XLF on NHEJ are direct. We identified XLF in a yeast two-hybrid screen for XRCC4 binding proteins and subsequently verified this interaction by biochemical means. Furthermore, we have found that XLF not only forms part of this complex but is predicted to display structural similarity to XRCC4. Based on these findings, it seems reasonable to conclude that XLF promotes NHEJ at least in part by regulating the activity of the XRCC4-Ligase IV complex. In line with this prediction, siRNA-mediated downregulation of XLF yields radiosensitivity and NHEJ defects that are at least as strong as those generated by depletion of XRCC4.

How might XLF functionally cooperate with the XRCC4-Ligase IV complex? While it is possible that XLF regulates the stability or nuclear localization of XRCC4 and/or Ligase IV, we feel that this is unlikely because XRCC4 and Ligase IV are still detected in the nucleus of XLF-deficient 2BN cells (P.A., unpublished data). Instead, we favor a model in which XLF promotes the DNA ligation function of the XRCC4-Ligase IV complex. One attractive scenario, suggested by the predicted structural homologies between XRCC4 and XLF, is that XRCC4 principally functions with Ligase IV not as an XRCC4 homomultimer but as an XRCC4-XLF heteromultimer. Such a model would be consistent with the observation that XRCC4, although essential for NHEJ in vivo, only modestly enhances Ligase IV activity in vitro (Grawunder et al., 1997; Modesti et al., 1999). It will hence be interesting to study the effects of XLF on Ligase IV activity both in the absence or presence of XRCC4. Nevertheless, it is important to note that XRCC4 and Ligase IV seem to be present at higher levels in cells than XLF; and indeed, while we have found that XLF is tightly associated with the XRCC4 complex in immunoprecipitation studies, not all cellular XRCC4 appears to be bound to XLF (Figure 2). Supporting these observations, we found that XLF cofractionates with a proportion of XRCC4 and Ligase IV upon size-exclusion chromatography at approximately 200 kDa (P.A., unpublished data), supporting a model where XRCC4 (~38 kDa), XLF (~33 kDa), and Ligase IV (~103 kDa) form one complex with the previously described XRCC4:Ligase IV stochiometry of 2:1 (Modesti et al., 2003). However, in these studies we have also observed another population of XRCC4 and Ligase IV that fractionates in higher-order complexes that are apparently XLF free. In this regard, it is noteworthy that previous structural studies on XRCC4 have indicated its potential to exist in both dimeric and tetrameric states (Critchlow et al., 1997; Junop et al., 2000; Lee et al., 2000; Modesti et al., 2003) and that there are reasons to suppose that the tetrameric XRCC4 state might be incompatible with the NHEJ functionality of its complex with Ligase IV (Modesti et al., 2003; Sibanda et al., 2001). It is therefore tempting to speculate that XLF binding might alter the equilibrium between the two multimeric states of XRCC4, thus controlling Ligase IV activity. In regard to these models, it will clearly be of interest to determine the crystal structure of XLF both alone and in association with XRCC4. Alternatively, or in addition, XLF might regulate the access of the XRCC4-Ligase IV complex to DNA lesions. In vitro XRCC4-Ligase IV does not preferentially bind to its substrate, DNA ends, but has been shown to cooperatively bind to large DNA fragments (Modesti et al., 1999). XLF could therefore be required for XRCC4-Ligase IV recruitment to DNA ends or could mediate recruitment, for example by bridging the complex to other NHEJ components such as Ku and DNA-PKcs. Recently, an elegant in vitro NHEJ system has been developed in which XRCC4- and Ligase IV-dependent end-joining takes place in the absence of XLF (Ma et al., 2004). It will be of interest to see whether the inclusion of XLF increases the NHEJ efficiency of such systems.

A key conclusion arising from our work is that an *XLF* mutation causes the radiosensitivity and NHEJ defects of 2BN cells, which are derived from a radiosensitive immune-deficient patient. This mutation leads to a translational frameshift at codon four in the *XLF* open reading frame, meaning that the protein translated from this mRNA would be severely

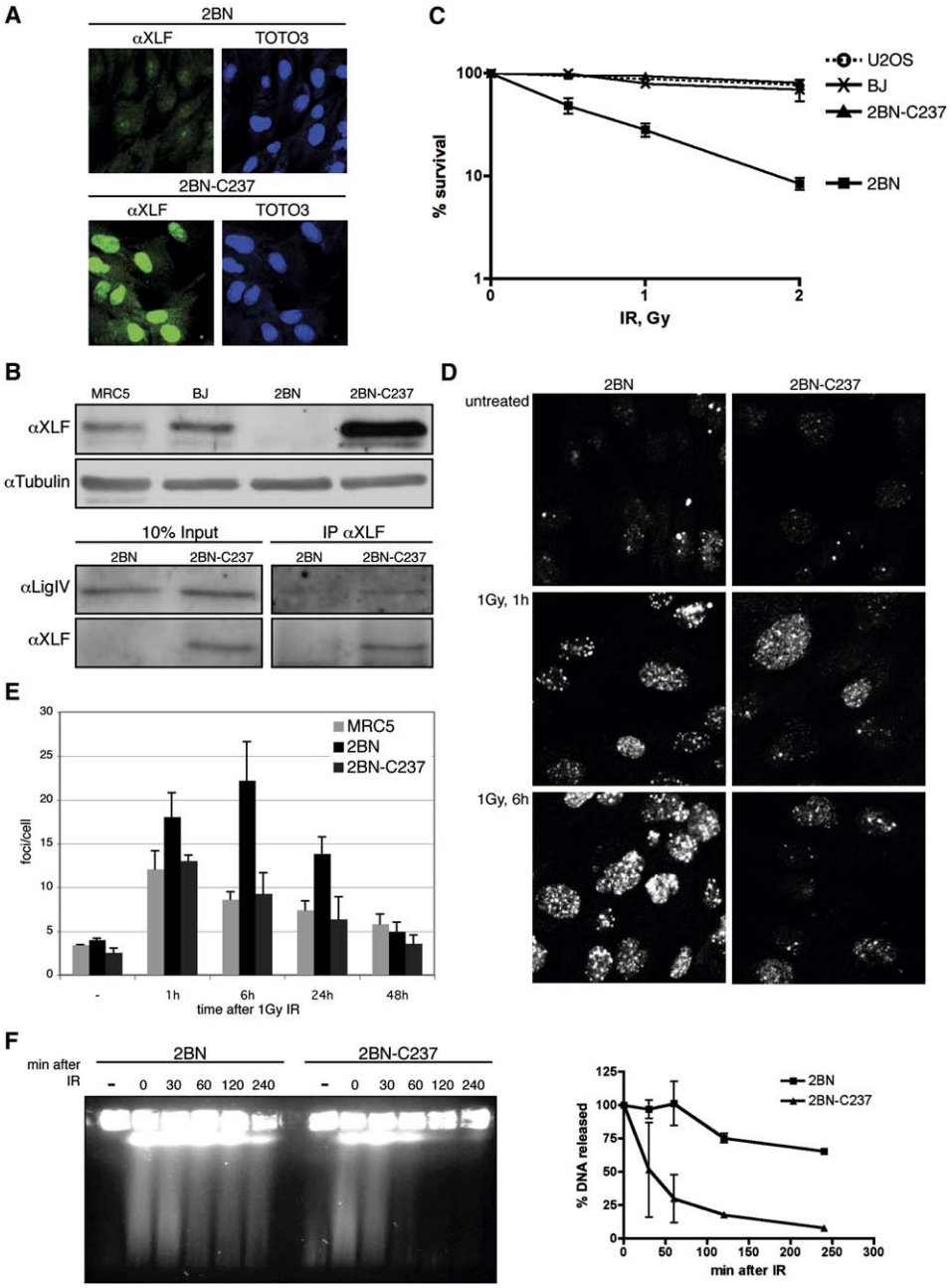

Figure 5. Reintroduction of Wild-Type XLF into 2BN Cells Eliminates Their Radiosensitivity and DSB Repair Defects

(A) Generation of a cell line derived from 2BN (clone 2BN-C237), where XLF was stably reintroduced into the genome, leads to the expression of nuclear XLF protein. Immunofluorescence microscopy of 2BN (top) and XLF complemented 2BN-C237 (bottom) cells. Cells were stained with rabbit anti-XLF antibody and TOTO3.

(B) XLF in 2BN-C237 cells interacts with Ligase IV. Top: immunoblot analysis of extracts prepared from MRC5, BJ, 2BN, and XLF complemented 2BN-C237 cells. Bottom: coimmunoprecipitation of Ligase IV with XLF. XLF was precipitated from 500 μg of 2BN-C237 or 2BN extract with rabbit anti-XLF antibody. Samples were analyzed by immunoblotting with rabbit anti-Ligase IV and rabbit anti-XLF antibody, as indicated. To prevent unspecific crossreactions between the rabbit antibodies, HRP-conjugated protein A was used as secondary reagent. Ten percent of input material was analyzed as a control.

(C) Cell lines derived from 2BN complemented with XLF are no longer radiosensitive. Clonogenic survival of 2BN (■), 2BN-C237 (▲), BJ (X), and U2OS (○) cells. Cells were treated with the indicated doses of IR. Data represent the mean and standard deviation of three independent experiments. For sake of clarity, complemented 2BN-231 cells were omitted as they show identical survival to 2BN-237.

(D) Complementation of the DSB repair defect of 2BN cells by XLF, as measured by γH2AX foci formation. 2BN cells or complemented 2BN-C237 cells were immunostained with anti-histone phospho-Ser 139 antibodies before or at the indicated times after treatment with 1Gy of IR.

truncated and would lack all of the evolutionarily conserved regions of the protein. On face value, this suggests strongly that 2BN cells and the patient from which they were derived possess a fully inactivating mutation in the *XLF* gene; and in line with this idea, we have been unable to detect XLF protein expression in 2BN cells even when using the most sensitive detection systems available. While these conclusions are not a priori in conflict with current models for the physiological functions of the NHEJ apparatus, the fact that the radiosensitive patient giving rise to 2BN cells was overtly normal with only mild developmental delay (Dai et al., 2003; P. Jeggo, personal communication) is surprising in light of the general consensus that full NHEJ deficiency is likely to be incompatible with human viability. Indeed, despite targeted searches, no loss-of-function mutations in the genes for Ligase IV or XRCC4 have so far been described in human patients. Furthermore, although several radiosensitive patients have been identified bearing mutations in the gene for Ligase IV, in all cases these appear to be hypomorphic conditions, with the severity of the patient phenotype broadly reflecting the extent to which Ligase IV function is disabled (O'Driscoll et al., 2001). In addition, while the gene for Ligase IV has been homozygously inactivated in a human pre-B cell line to yield radiosensitive but viable cells (Grawunder et al., 1998a), inactivation of the gene for XRCC4 or DNA Ligase IV leads to early embryonic lethality in the mouse, at least in part due to extensive apoptosis of newly generated postmitotic neurons in the developing nervous system (for review, see Ferguson and Alt [2001]).

One possible explanation for the lack of lethality of the 2BN mutation in man, therefore, is that the core NHEJ apparatus is in fact not essential for mammalian viability. Support for this idea is provided by the fact that components of the Ku-DNA-PKcs complex, otherwise central to NHEJ, are not required for viability in the mouse (for example, see Gu et al. [1997], Nussenzweig et al. [1996], and Taccioli et al. [1998]). Alternatively, it is possible that NHEJ is indeed needed for mammalian viability but that the only really essential components of this pathway are XRCC4 and Ligase IV. Finally, we note that we cannot at the present time rule out the possibility that the 2BN mutation does not totally inactivate XLF activity and that some XLF protein with residual function is made from alternative, downstream translational initiation codons in the mutated mRNA. Formal demonstration of whether or not XLF is needed for mammalian survival will await the generation of knockout mice.

Over the past decade, it has become increasingly apparent that inherited defects in DSB repair components can be associated with enhanced predisposition to cancer, and that such deficiencies—or somatically acquired mutations or epigenetic silencing of the genes for DSB repair factors—can affect the responses of patients and their tumors toward radiotherapy and DNA-damaging chemotherapies. Although the patient yielding the 2BN cells provides an extreme example of radiation hypersensitivity arising from a defect in DSB repair, it is tempting to speculate that more subtle mutations or polymorphisms in XLF and other NHEJ components will affect radiotherapy outcome at the more subtle level. Finally, we note that loss or variation in XLF activity might contribute toward cancer predisposition in the wider population.

EXPERIMENTAL PROCEDURES

Plasmids

GST-XLF was created by PCR cloning in pGEX-4-TKP (Amersham), GFP-XLF, FLAG-XLF, and HA-XLF were generated by PCR cloning into pCDNA3.1^{+} (Invitrogen). For creation of the stable XLF complemented cell line, full-length XLF was cloned in pBABE-puro.

Extract Preparation, Protein Expression, and Purifications

Mammalian whole-cell extracts were prepared in SDS sample buffer, RIPA buffer, or EBC buffer (50 mM Tris-HCl [pH 7.5]; 120 mM NaCl; 0.5% NP-40; 1 mM dithiothreitol; 1 mM AEBSF; 1 mM NaF; 1 mM β-glycerophosphate; 10 μg/ml Leupeptin). HNE was from Computer Cell Culture Center. Recombinant XLF protein was synthesized in *E. coli* BL21 (Novagen) and was purified to near homogeneity by glutathione Sepharose affinity chromatography (Amersham).

GST Pull-Downs and Immunoprecipitations

Immunoprecipitations and GST pull-downs were done as described before (Goldberg et al., 2003). Recombinant GST-XLF bound to glutathione Sepharose (Amersham) was incubated with precleared HNE for 4 hr in the presence of 50 μg/ml ethidium bromide and washed five times with EBC buffer before resuspension in SDS sample buffer. Immunoprecipitations were done with Protein A and Protein G Sepharose for rabbit polyclonal and mouse monoclonal antibodies, respectively. Lysates including 20 μg/ml ethidium bromide were precleared with the respective beads and subsequently incubated overnight with 1 μg of antibody (or 1 μl of serum). Complexes were precipitated with beads for 1 hr and washed five times with EBS buffer before resuspension in SDS sample buffer.

RT-PCR and Genomic Sequencing

Total RNA was prepared using High Pure RNA Isolation Kit (Roche) according to manufacturer's instructions. cDNA was synthesized using the cDNA synthesis kit (Roche) according to manufacturer's instructions. Total genomic DNA was prepared by boiling lysis. PCR reactions were carried out using the High Fidelity PCR Kit (Roche). PCR products were sequenced directly as well as cloned into pCR-Blunt II-Topo (Invitrogen) to improve reading. Sequencing reactions were done by the Department of Biochemistry DNA sequencing facility (Cambridge, United Kingdom).

Yeast Two-Hybrid Screen

Yeast-two hybrid screening was performed with pLexA-dir encoding full-length XRCC4 as a bait construct, screening a pACT2 human brain library (complexity: 3.5E6). The screen was carried out in collaboration with Dualsystems (Zurich, Switzerland).

(E) Complementation of 2BN cells with XLF changes the kinetics of H2AX phosphorylation back to that of wild-type cells. Statistical analysis of phospho-H2A foci formation in MRC5, 2BN, and 2BN-C237 cells at the indicated time points after 1 Gy of IR treatment. At least 100 cells were counted per time point, and the data represent mean and standard deviation of two independent experiments.

(F) Complementation of 2BN cells with XLF eliminates their defect in chromosomal DSB repair. PFGE of 2BN and 2BN-C237 cells. Cells were irradiated for 40 min at 1.8 Gy/min on ice and left for the indicated amount of time to repair at 37ºC. Then ~100,000 cells were loaded per well and the gel was run at 33V, 50–5000 s linear switch time for 66 hr. Left: representative ethidium bromide-stained gel. Right: released DNA was quantified by using MacBAS image analysis. Data represent percentage of DNA released relative to DNA release directly after irradiation. Error bars represent mean and standard deviation of two independent experiments.

Cell Culture

293T and U2OS cells were cultured in DMEM containing 10% serum. 2BNhTERT (2BN, a gift from P. Jeggo; Dai et al., 2003), 2BN-C237, 2BN-C231, MRC5hTERT (MRC5), and BJhTERT (BJ) cells were cultured in DMEM containing 15% serum. Complementation of 2BN cells was done by transfection of linearized pBabe-puro plasmid encoding wild-type XLF, followed by selection with puromycin. Single-cell colonies were isolated and expanded. Transfection of plasmids and siRNA duplexes was done with either FuGene6 (Roche) or calcium phosphate and oligofectamine (Invitrogen), respectively. The luciferase- (CGUACGCGGAAUACUUCGAdTdT) and GFP-targeting (GGCUACGUCCAGGAGCGCACCdTdT) siRNA duplexes were from Dharmacon. XLF (1, GCAUUACAGUGCCAAGUGAdTdT), (2, CGCUGAUUCGAGAUCGAUUGAdTdT) and XRCC4 (AUAUGUUGGUGAACUGAGAdTdT) targeting siRNA duplexes were synthesized by MWG-Biotech. X-ray irradiation and clonogenic survival assays were done as previously described (Goldberg et al., 2003). Random plasmid integration was done by transfection of linearized pEYFP-Nuc expression plasmid. Twenty-four hours later, cells were replated at low density in G418-containing medium, and colonies were counted 10 days after transfection. A fraction of the transfected cells was monitored for nuclear YFP expression to normalize the data for transfection efficiency.

Antibodies and Immunofluorescence

Commercial antibodies used in this study were from Abcam (XRCC4, Tubulin), Upstate (γH2AX), SIGMA (anti-FLAG M2, rabbit anti-HA), Roche (HA-Peroxidase 3F10), and Genetex (mouse XRCC4). Monoclonal anti-GFP and anti-HA antibodies were from Cancer Research UK. Rabbit antiserum recognizing human Ligase IV and MRE11 have been described before (Critchlow et al., 1997; Goldberg et al., 2003). Anti-human-XLF antibody was raised for this study against purified recombinant GST-XLF, characterized, and affinity purified. For immunofluorescence staining, cells were grown on glass coverslips and fixed in 3.5% paraformaldehyde for 12 min. Fixed cells were washed briefly with PBS + 0.5% Triton-X100 and stained with antibodies as indicated. Analysis of IRIF was performed as described before (Goldberg et al., 2003; Kuhne et al., 2004). At least 100 cells were scored per time point per experiment.

Pulsed-Field Gel Electrophoresis

PFGE was done as described before (Kuhne et al., 2004). Cells were harvested and ~100,000 cells were embedded in 0.5% low-melting agarose. Plugs were incubated overnight at 55ºC in 500 μl lysis buffer (50 mM Tris [pH 8.0], 50 mM EDTA [pH 8.0], 2% sarcosyl, 2 mg/ml proteinase) and washed twice with 1 ml of TE at room temperature. Electrophoresis of the prepared samples was performed using the Gene NavigatorTM system (Amersham Biosciences). Electrophoretic conditions were as indicated.

Supplemental Data

Supplemental Data include one figure and one table and can be found with this article online at http://www.cell.com/cgi/content/full/124/2/301/DC1/.

ACKNOWLEDGMENTS

We thank P. Jeggo for generously providing us with 2BN cells. We also thank all members of SPJ laboratory for their support and advice, particularly A. Sartori, M. Stucki, J. Falck, and J. Coates. We also thank A. Doherty and P. Jeggo for helpful discussions and A. Sartori for critical reading of the manuscript. This work was supported by grants from Cancer Research UK and was made possible by core-infrastructure funding provided by Cancer Research UK and the Wellcome Trust. P.A. is supported by a Cancer Research UK Studentship.

Received: November 28, 2005
Revised: December 20, 2005
Accepted: December 28, 2005
Published: January 26, 2006

REFERENCES

Barnes, D.E., Stamp, G., Rosewell, I., Denzel, A., and Lindahl, T. (1998). Targeted disruption of the gene encoding DNA ligase IV leads to lethality in embryonic mice. Curr. Biol. *8*, 1395–1398.

Bryans, M., Valenzano, M.C., and Stamato, T.D. (1999). Absence of DNA ligase IV protein in XR-1 cells: evidence for stabilization by XRCC4. Mut. Res. *433*, 53–58.

Buck, D., Malivert, L., de Chasseval, R., Barraud, A., Fondaneche, M.-C., Sanal, O., Plebani, A., Stephan, J.-L., Hufnagel, M., le Deist, F., et al. (2006). Cernunnos, a novel nonhomologous end-joining factor, is mutated in human immunodeficiency with microcephaly. Cell *124*, this issue, 287–299.

Chappell, C., Hanakahi, L.A., Karimi-Busheri, F., Weinfeld, M., and West, S.C. (2002). Involvement of human polynucleotide kinase in double-strand break repair by non-homologous end joining. EMBO J. *21*, 2827–2832.

Chen, L., Trujillo, K., Sung, P., and Tomkinson, A.E. (2000). Interactions of the DNA ligase IV–XRCC4 complex with DNA ends and the DNA-dependent protein kinase. J. Biol. Chem. *275*, 26196–26205.

Clements, P.M., Breslin, C., Deeks, E.D., Byrd, P.J., Ju, L., Bieganowski, P., Brenner, C., Moreira, M.C., Taylor, A.M., and Caldecott, K.W. (2004). The ataxia-oculomotor apraxia 1 gene product has a role distinct from ATM and interacts with the DNA strand break repair proteins XRCC1 and XRCC4. DNA Repair (Amst.) *3*, 1493–1502.

Critchlow, S.E., Bowater, R.P., and Jackson, S.P. (1997). Mammalian DNA double-strand break repair protein XRCC4 interacts with DNA ligase IV. Curr. Biol. *7*, 588–598.

Dai, Y., Kysela, B., Hanakahi, L.A., Manolis, K., Riballo, E., Stumm, M., Harville, T.O., West, S.C., Oettinger, M.A., and Jeggo, P.A. (2003). Nonhomologous end joining and V(D)J recombination require an additional factor. Proc. Natl. Acad. Sci. USA *100*, 2462–2467.

Difilippantonio, M.J., Petersen, S., Chen, H.T., Johnson, R., Jasin, M., Kanaar, R., Ried, T., and Nussenzweig, A. (2002). Evidence for replicative repair of DNA double-strand breaks leading to oncogenic translocation and gene amplification. J. Exp. Med. *196*, 469–480.

Ferguson, D.O., and Alt, F.W. (2001). DNA double strand break repair and chromosomal translocation: lessons from animal models. Oncogene *20*, 5572–5579.

Frank, K.M., Sekiguchi, J.M., Seidl, K.J., Swat, W., Rathbun, G.A., Cheng, H.-L., Davidson, L., Kangaloo, L., and Alt, F.W. (1998). Late embryonic lethality and impaired V(D)J recombination in mice lacking DNA ligase IV. Nature *396*, 173–177.

Gellert, M. (2002). V(D)J recombination: RAG proteins, repair factors, and regulation. Annu. Rev. Biochem. *71*, 101–132.

Goldberg, M., Stucki, M., Falck, J., D'Amours, D., Rahman, D., Pappin, D., Bartek, J., and Jackson, S.P. (2003). MDC1 is required for the intra-S-phase DNA damage checkpoint. Nature *421*, 952–956.

Grawunder, U., Wilm, M., Wu, X., Kulesza, P., Wilson, T.E., Mann, M., and Lieber, M.R. (1997). Activity of DNA ligase IV stimulated by complex formation with XRCC4 protein in mammalian cells. Nature *388*, 492–495.

Grawunder, U., Zimmer, D., Fugmann, S., Schwarz, K., and Lieber, M.R. (1998a). DNA ligase IV is essential for V(D)J recombination and DNA double-strand break repair in human precursor lymphocytes. Mol. Cell *2*, 477–484.

Grawunder, U., Zimmer, D., and Lieber, M.R. (1998b). DNA ligase IV binds to XRCC4 via a motif located between rather than within its BRCT domains. Curr. Biol. *8*, 873–876.

Gu, Y., Seidl, K.J., Rathbun, G.A., Zhu, C., Manis, J.P., van der Stoep, N., Davidson, L., Cheng, H.-L., Sekiguchi, J.M., Frank, K., et al. (1997). Growth retardation and leaky SCID phenotype of Ku70-deficient mice. Immunity *7*, 653–665.

Haber, J.E. (2000). Partners and pathways—repairing a double-strand break. Trends Genet. *16*, 259–264.

Hefferin, M.L., and Tomkinson, A.E. (2005). Mechanism of DNA double-strand break repair by non-homologous end joining. DNA Repair (Amst.) *4*, 639–648.

Herrmann, G., Lindahl, T., and Schar, P. (1998). *Saccharomyces cerevisiae* LIF1: a function involved in DNA double-strand break repair related to mammalian XRCC4. EMBO J. *17*, 4188–4198.

Hsu, H.-L., Yannone, S.M., and Chen, D.J. (2002). Defining interactions between DNA-PK and ligase IV/XRCC4. DNA Repair (Amst.) *1*, 225–235.

Iliakis, G., Wang, H., Perrault, A.R., Boecker, W., Rosidi, B., Windhofer, F., Wu, W., Guan, J., Terzoudi, G., and Pantelias, G. (2004). Mechanisms of DNA double strand break repair and chromosome aberration formation. Cytogenet. Genome Res. *104*, 14–20.

Junop, M.S., Modesti, M., Guarné, A., Ghirlando, R., Gellert, M., and Yang, W. (2000). Crystal structure of the Xrcc4 DNA repair protein and implications for end joining. EMBO J. *19*, 5962–5970.

Kelley, L.A., MacCallum, R.M., and Sternberg, M.J. (2000). Enhanced genome annotation using structural profiles in the program 3D-PSSM. J. Mol. Biol. *299*, 499–520.

Khanna, K.K., and Jackson, S.P. (2001). DNA double-strand breaks: signaling, repair and the cancer connection. Nat. Genet. *27*, 247–254.

Koch, C.A., Agyei, R., Galicia, S., Metalnikov, P., O'Donnell, P., Starostine, A., Weinfeld, M., and Durocher, D. (2004). Xrcc4 physically links DNA end processing by polynucleotide kinase to DNA ligation by DNA ligase IV. EMBO J. *23*, 3874–3885.

Kuhne, M., Riballo, E., Rief, N., Rothkamm, K., Jeggo, P.A., and Lobrich, M. (2004). A double-strand break repair defect in ATM-deficient cells contributes to radiosensitivity. Cancer Res. *64*, 500–508.

Kysela, B., Doherty, A.J., Chovanec, M., Stiff, T., Ameer-Beg, S.M., Vojnovic, B., Girard, P.M., and Jeggo, P.A. (2003). Ku stimulation of DNA ligase IV-dependent ligation requires inward movement along the DNA molecule. J. Biol. Chem. *278*, 22466–22474.

Leber, R., Wise, T.W., Mizuta, R., and Meek, K. (1998). The *XRCC4* gene product is a target for and interacts with the DNA-dependent protein kinase. J. Biol. Chem. *273*, 1794–1801.

Lee, K.-J., Huang, J., Takeda, Y., and Dynan, W.S. (2000). DNA ligase IV and XRCC4 form a stable mixed tetramer that functions synergistically with other repair factors in a cell-free end-joining system. J. Biol. Chem. *275*, 34787–34796.

Li, Z., Otevrel, T., Gao, Y., Cheng, H.-L., Seed, B., Stamato, T.D., Taccioli, G.E., and Alt, F.W. (1995). The *XRCC4* gene encodes a novel protein involved in DNA double-strand break repair and V(D)J recombination. Cell *83*, 1079–1089.

Lieber, M.R., Ma, Y., Pannicke, U., and Schwarz, K. (2003). Mechanism and regulation of human non-homologous DNA end-joining. Nat. Rev. Mol. Cell Biol. *4*, 712–720.

Lieber, M.R., Ma, Y., Pannicke, U., and Schwarz, K. (2004). The mechanism of vertebrate nonhomologous DNA end joining and its role in V(D)J recombination. DNA Repair (Amst.) *3*, 817–826.

Lou, Z., Chen, B.P., Asaithamby, A., Minter-Dykhouse, K., Chen, D.J., and Chen, J. (2004). MDC1 regulates DNA-PK autophosphorylation in response to DNA damage. J. Biol. Chem. *279*, 46359–46362.

Ma, Y., Lu, H., Tippin, B., Goodman, M.F., Shimazaki, N., Koiwai, O., Hsieh, C.L., Schwarz, K., and Lieber, M.R. (2004). A biochemically defined system for mammalian nonhomologous DNA end joining. Mol. Cell *16*, 701–713.

McElhinny, S.A.N., Snowden, C.M., McCarville, J., and Ramsden, D.A. (2000). Ku recruits the XRCC4-ligase IV complex to DNA ends. Mol. Cell. Biol. *20*, 2996–3003.

Mills, K.D., Ferguson, D.O., and Alt, F.W. (2003). The role of DNA breaks in genomic instability and tumorigenesis. Immunol. Rev. *194*, 77–95.

Mirzoeva, O.K., and Petrini, J.H.J. (2001). DNA damage-dependent nuclear dynamics of the Mre11 complex. Mol. Cell. Biol. *21*, 281–288.

Modesti, M., and Kanaar, R. (2001). Homologous recombination: from model organisms to human disease. Genome Biol. *2*, R1014.

Modesti, M., Hesse, J.E., and Gellert, M. (1999). DNA binding of Xrcc4 protein is associated with V(D)J recombination but not with stimulation of DNA ligase IV activity. EMBO J. *18*, 2008–2018.

Modesti, M., Junop, M.S., Ghirlando, R., van de Rakt, M., Gellert, M., Yang, W., and Kanaar, R. (2003). Tetramerization and DNA ligase IV interaction of the DNA double-strand break repair protein XRCC4 are mutually exclusive. J. Mol. Biol. *334*, 215–228.

Moshous, D., Callebaut, I., de Chasseval, R., Corneo, B., Cavazzana-Calvo, M., Le Deist, F., Tezcan, I., Sanal, O., Bertrand, Y., Philippe, N., et al. (2001). Artemis, a novel DNA double-strand break repair/V(D)J recombination protein, is mutated in human severe combined immune deficiency. Cell *105*, 177–186.

Nussenzweig, A., Chen, C., da Costa Soares, V., Sanchez, M., Sokol, K., Nussenzweig, M.C., and Li, G.C. (1996). Requirement for Ku80 in growth and immunoglobulin V(D)J recombination. Nature *382*, 551–555.

O'Driscoll, M., Cerosaletti, K.M., Girard, P.M., Dai, Y., Stumm, M., Kysela, B., Hirsch, B., Gennery, A., Palmer, S.E., Seidel, J., et al. (2001). DNA ligase IV mutations identified in patients exhibiting developmental delay and immunodeficiency. Mol. Cell *8*, 1175–1185.

Riballo, E., Critchlow, S.E., Teo, S.-H., Doherty, A.J., Priestley, A., Broughton, B., Kysela, B., Beamish, H., Plowman, N., Arlett, C.F., et al. (1999). Identification of a defect in DNA ligase IV in a radiosensitive leukaemia patient. Curr. Biol. *9*, 699–702.

Rich, T., Allen, R.L., and Wyllie, A.H. (2000). Defying death after DNA damage. Nature *407*, 777–783.

Rogakou, E.P., Pilch, D.R., Orr, A.H., Ivanova, V.S., and Bonner, W.M. (1998). DNA double-stranded breaks induce histone H2AX phosphorylation on serine 139. J. Biol. Chem. *273*, 5858–5868.

Robins, P., and Lindahl, T. (1996). DNA ligase IV from HeLa cell nuclei. J. Biol. Chem. *271*, 24257–24261.

Rothkamm, K., and Lobrich, M. (2003). Evidence for a lack of DNA double-strand break repair in human cells exposed to very low x-ray doses. Proc. Natl. Acad. Sci. USA *100*, 5057–5062.

Shi, J., Blundell, T.L., and Mizuguchi, K. (2001). FUGUE: sequence-structure homology recognition using environment-specific substitution tables and structure-dependent gap penalties. J. Mol. Biol. *310*, 243–257.

Sibanda, B.L., Critchlow, S.E., Begun, J., Pei, X.Y., Jackson, S.P., Blundell, T.L., and Pellegrini, L. (2001). Crystal structure of an Xrcc4–DNA ligase IV complex. Nat. Struct. Biol. *8*, 1015–1019.

Smith, G.C.M., and Jackson, S.P. (1999). The DNA-dependent protein kinase. Genes Dev. *13*, 916–934.

Taccioli, G.E., Amatucci, A.G., Beamish, H.J., Gell, D., Xiang, X.H., Arzayus, M.I.T., Priestley, A., Jackson, S.P., Rothstein, A.M., Jeggo, P.A., and Herrera, V.L.M. (1998). Targeted disruption of the catalytic subunit of the DNA-PK gene in mice confers severe combined immunodeficiency and radiosensitivity. Immunity *9*, 355–366.

Teo, S.-H., and Jackson, S.P. (2000). Lif1p targets the DNA ligase Lig4p to sites of DNA double-strand breaks. Curr. Biol. *10*, 165–168.

Wang, H., Rosidi, B., Perrault, R., Wang, M., Zhang, L., Windhofer, F., and Iliakis, G. (2005). DNA ligase III as a candidate component of backup pathways of nonhomologous end joining. Cancer Res. *65*, 4020–4030.

West, S.C. (2003). Molecular views of recombination proteins and their control. Nat. Rev. Mol. Cell Biol. *4*, 435–445.

Weterings, E., and Van Gent, D.C. (2004). The mechanism of non-homologous end-joining: a synopsis of synapsis. DNA Repair (Amst.) *3*, 1425–1435.